

# Bayesian Neural Networks for Reversible Steganography

Ching-Chun Chang

**Abstract**—Recent advances in deep learning have led to a paradigm shift in reversible steganography. A fundamental pillar of reversible steganography is predictive modelling which can be realised via deep neural networks. However, non-trivial errors exist in inferences about some out-of-distribution and noisy data. In view of this issue, we propose to consider uncertainty in predictive models based upon a theoretical framework of Bayesian deep learning. Bayesian neural networks can be regarded as self-aware machinery; that is, a machine that knows its own limitations. To quantify uncertainty, we approximate the posterior predictive distribution through Monte Carlo sampling with stochastic forward passes. We further show that predictive uncertainty can be disentangled into aleatoric and epistemic uncertainties and these quantities can be learnt in an unsupervised manner. Experimental results demonstrate an improvement delivered by Bayesian uncertainty analysis upon steganographic capacity-distortion performance.

**Index Terms**—Bayesian neural networks, predictive modelling, reversible steganography, uncertainty quantification.

## I. INTRODUCTION

ARTIFICIAL intelligence arises from the question ‘Can machines think?’ [1]. Machine learning refocuses attention on addressing solvable problems of a practical nature automatically. Deep learning is a subclass of machine-learning algorithms based on neural networks and connectionism [2]–[4]. Most modern deep-learning models are regarded as *deterministic* as they only offer predictions but lacking confidence bounds for data analysis and decision making, thereby incurring risks in automated systems. As a safety concern, it is important to be aware of the limitations of a machine that is deployed in real-world settings and granted autonomous control [5]. While the notion of machine consciousness is illusive and there is no indication that contemporary artificial intelligence is anywhere close to engendering that, uncertainty quantification would be a principle element towards self-aware machinery. Bayesian deep learning provides a way to calculate uncertainty based on a *probabilistic* conception [6].

Digital steganography is the practice of covering messages within digital media [7]. Although steganographic distortion is generally imperceptible, *reversibility* is a necessity for applications in which data integrity is of major priority [8]–[12]. The recent development of deep learning has brought a paradigm shift in the research of reversible steganography [13]–[16]. Similar to lossless compression [17], predictive modelling forms a fundamental pillar of reversible steganography for analysing redundancy in digital signals [18]–[22]. It has been

reported that deep neural networks can serve the role of predictive models [23]–[25]. Despite an improved accuracy offered by neural networks, non-trivial prediction errors occur when making inferences about some *out-of-distribution* and *noisy* test data.

In this letter, we study uncertainty in predictive neural networks for reversible steganography based on a theoretical framework of Bayesian deep learning [26]. Our objective is to develop a learning-based method for analysing and quantifying uncertainty due to out-of-distribution and noisy data, hence improving steganographic capacity-distortion performance.

## II. METHODOLOGY

We begin by formulating a reversible steganographic scheme that incorporates a Bayesian neural network and then present a derivation of uncertainty.

### A. Reversible Steganography

Reversible steganography considers the following scenario. A sender communicates a message to a receiver by introducing removable modifications to a carrier signal. We refer to the original signal as the *cover* and the modified counterpart as the *stego*. Residual modulation is a conventional technique for hiding messages within digital images in a reversible fashion. We propose a simple scheme based on residual modulation for incorporating a Bayesian neural network (BNN) with a schematic workflow illustrated in Figure 1. In the preliminary phase, pixels of an image are divided into a *context* set and a *query* set, denoted respectively by  $\mathbf{x}$  and  $\mathbf{y}$ . A BNN is then deployed to predict the intensity of each query pixel as well as to estimate the inherent variance in data based on the given contextual information:

$$\{\hat{\mathbf{y}}, \boldsymbol{\sigma}^2\} = \text{BNN}(\mathbf{x}). \quad (1)$$

For the time being, we assume an uncertainty map is derived from either/both  $\hat{\mathbf{y}}$  or/and  $\boldsymbol{\sigma}^2$ . The map indicates an estimated uncertainty over the prediction for each pixel and provides guidance on message embedding. Residual modulation is premised on a statistical principle (i.e. *law of error*) that residuals generally centre around zero and the frequency of a residual is inversely proportional to its magnitude [27]. It assigns residuals of small magnitude (thresholded by a parameter  $\alpha$ ) as the *stego channel* to carry the payload at the expense of causing greater distortion to large residuals. Based on a supposition that the expected residual magnitude can be captured by the uncertainty map, we can modulate the residuals along ascending uncertainty or alternatively sort them

C.-C. Chang is with the University of Warwick, Coventry, UK (email: c.c.chang@warwickgrad.net).

Digital Object Identifier xx.xxxx/2022

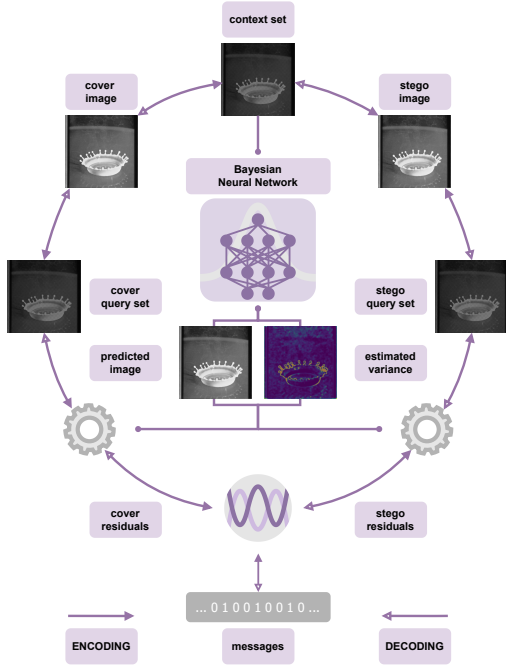


Fig. 1: Workflow of reversible steganography with BNN.

by ascending uncertainty prior to modulation, rendering an optimal embedding pathway. In the encoding phase, residuals are computed by  $\epsilon = \mathbf{y} - \hat{\mathbf{y}}$ . Message bits are embedded by modulating the residuals via a reversible coding algorithm, causing recoverable distortion to the residuals:

$$\epsilon' = \text{modulate}(\epsilon, \mathbf{m}). \quad (2)$$

The modulated residuals are added to the predicted intensities, resulting in a stego query set  $\mathbf{y}' = \hat{\mathbf{y}} + \epsilon'$ . Message extraction and image restoration are performed in a similar manner. To begin with, the procedures in the preliminary phase are carried out, yielding the same results since the contextual information remains intact. In the decoding phase, the embedding order is identified in accordance with the uncertainty map and the residuals are computed by  $\epsilon' = \mathbf{y}' - \hat{\mathbf{y}}$ . These residuals are demodulated to extract the message and to revert the residuals to their pristine state based on the corresponding reversible coding algorithm:

$$\{\epsilon, \mathbf{m}\} = \text{demodulate}(\epsilon'). \quad (3)$$

Finally, the original image is recovered by  $\mathbf{y} = \hat{\mathbf{y}} + \epsilon$ .

### B. Bayesian Inference

A neural network is a non-linear function that maps an input and model parameters to an output:

$$\mathbf{y} = f(\mathbf{x}, \theta) + \epsilon, \quad (4)$$

where  $\epsilon \sim \mathcal{N}(\mathbf{0}, \sigma^2)$  is a Gaussian observation noise. The goal of this regression problem is to find latent model parameters  $\theta$  given the observed noisy data. Let us denote by  $\mathcal{X}$  the training inputs and by  $\mathcal{Y}$  the corresponding outputs. Bayesian inference provides a way to estimate uncertainty by deriving

the (posterior) *predictive distribution* of  $\mathbf{y}_*$  at a test input  $\mathbf{x}_*$  using the parameter posterior, as given by

$$p(\mathbf{y}_* | \mathbf{x}_*, \mathcal{X}, \mathcal{Y}) = \int \underbrace{p(\mathbf{y}_* | \mathbf{x}_*, \theta)}_{\text{likelihood}} \underbrace{p(\theta | \mathcal{X}, \mathcal{Y})}_{\text{posterior}} d\theta. \quad (5)$$

It takes into account of the posterior distribution over the model parameters  $\theta$ . Invoking the Bayes' theorem gives us the parameter posterior

$$p(\theta | \mathcal{X}, \mathcal{Y}) = \frac{\underbrace{p(\mathcal{Y} | \mathcal{X}, \theta)}_{\text{likelihood}} \cdot \underbrace{p(\theta)}_{\text{prior}}}{\underbrace{p(\mathcal{Y} | \mathcal{X})}_{\text{evidence}}}, \quad (6)$$

and we can assume a Gaussian prior and a Gaussian likelihood such that

$$\begin{aligned} \text{prior} \quad p(\theta) &= \mathcal{N}(\mathbf{0}, \mathbf{I}), \\ \text{likelihood} \quad p(\mathbf{y} | \mathbf{x}, \theta) &= \mathcal{N}(\mathbf{y} | \hat{\mathbf{y}}, \sigma^2). \end{aligned} \quad (7)$$

The denominator of the posterior is the marginal likelihood or model evidence, as defined by

$$p(\mathcal{Y} | \mathcal{X}) = \int \underbrace{p(\mathcal{Y} | \mathcal{X}, \theta)}_{\text{likelihood}} \underbrace{p(\theta)}_{\text{prior}} d\theta. \quad (8)$$

This integration is also referred to as *marginalisation* and the marginal likelihood can be regarded as the likelihood averaged over all possible parameter settings w.r.t. their plausibility. However, marginalisation is analytically intractable for deep-learning models and therefore we have to resort to approximation techniques.

### C. Monte Carlo Dropout

Variational inference is a technique for approximating intractable integrals in Bayesian inference [28]–[32]. Instead of evaluating the parameter posterior, we approximate it by a variational distribution  $q(\theta)$ , which belongs to a family of distributions of simpler form. By replacing  $p(\theta | \mathcal{X}, \mathcal{Y})$  with  $q(\theta)$  in the predictive distribution and approximating the integral with Monte Carlo integration, we derive that

$$\begin{aligned} p(\mathbf{y}_* | \mathbf{x}_*, \mathcal{X}, \mathcal{Y}) &\stackrel{\text{VI}}{\approx} \int p(\mathbf{y}_* | \mathbf{x}_*, \theta) q(\theta) d\theta \\ &\stackrel{\text{MC}}{\approx} \frac{1}{T} \sum_{t=1}^T p(\mathbf{y}_* | \mathbf{x}_*, \hat{\theta}_t), \end{aligned} \quad (9)$$

where  $\hat{\theta}_t \sim q(\theta)$ . Sampling model parameters from a variational distribution can be simulated by dropout [33], a stochastic process of multiplying the output of each neurone by a random variable drawn from a Bernoulli distribution [34]. In other words, each dropout configuration deactivates a portion of neurones, yielding a plausible realisation of the parametric model. Performing stochastic forward passes  $T$  times through a model with different dropout masks during the inference process is referred to as *Monte Carlo dropout* [35], as illustrated in Figure 2.

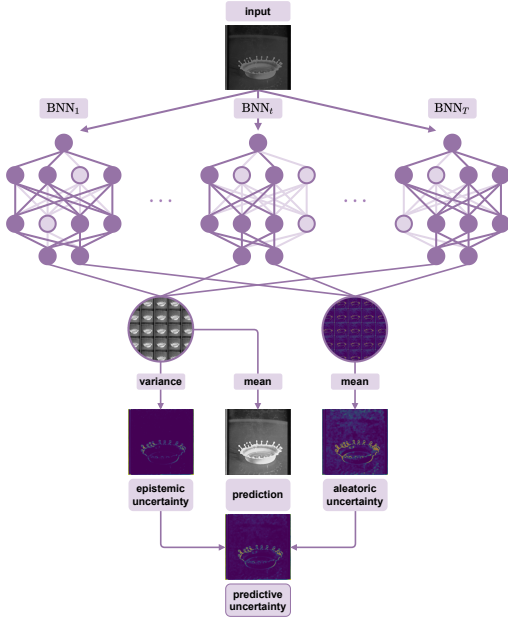


Fig. 2: Monte Carlo dropout as stochastic forward passes through BNN.

#### D. Uncertainty Disentanglement

A BNN offers a predictive distribution from which we can estimate the variance or *predictive uncertainty*. By the law of total variance, a variance can be decomposed into ‘unexplained’ and ‘explained’ components. This permits the disentanglement of *aleatoric* and *epistemic* uncertainties from predictive uncertainty [36]:

$$\mathbb{V}(\mathbf{y} | \mathbf{x}) = \underbrace{\mathbb{E}[\mathbb{V}(\mathbf{y} | \mathbf{x}, \boldsymbol{\theta})]}_{\text{aleatoric}} + \underbrace{\mathbb{V}(\mathbb{E}[\mathbf{y} | \mathbf{x}, \boldsymbol{\theta}])}_{\text{epistemic}}. \quad (10)$$

Aleatoric uncertainty captures randomness (or noise) inherent in the observations:

$$\mathbb{E}[\sigma^2] \approx \frac{1}{T} \sum_{t=1}^T \sigma_t^2. \quad (11)$$

Epistemic uncertainty occurs due to limited knowledge (or training data):

$$\begin{aligned} \mathbb{V}(\hat{\mathbf{y}}) &= \mathbb{E}[(\hat{\mathbf{y}} - \mathbb{E}[\hat{\mathbf{y}}])^2] = \mathbb{E}[\hat{\mathbf{y}}^2] - \mathbb{E}[\hat{\mathbf{y}}]^2 \\ &\approx \frac{1}{T} \sum_{t=1}^T \hat{\mathbf{y}}_t^2 - \left( \frac{1}{T} \sum_{t=1}^T \hat{\mathbf{y}}_t \right)^2. \end{aligned} \quad (12)$$

Hybrid predictive uncertainty can be computed by adding together aleatoric and epistemic uncertainties, each normalised with its sum. We perform dropout at test time and sample i.i.d. results  $\{\hat{\mathbf{y}}_t, \sigma_t^2\}_{t=1}^T \sim \text{BNN}_{\hat{\boldsymbol{\theta}}_t}(\mathbf{x})$  s.t.  $\hat{\boldsymbol{\theta}}_t \sim q^*(\boldsymbol{\theta})$ . The loss function for this *dual-headed* BNN is composed of a distance function  $\mathcal{D}$  and a regulariser  $\mathcal{R}$  balanced by  $\lambda$  [37], as given by

$$\mathcal{L}_{\text{BNN}} = \mathcal{D}(\mathbf{y}, \hat{\mathbf{y}}, \sigma^2) + \lambda \mathcal{R}(\sigma^2). \quad (13)$$

Let us denote by  $N$  the number of pixels in an image. The distance function is defined by

$$\mathcal{D} = \frac{1}{N} \sum_{n=1}^N (y_n - \hat{y}_n)^2 \left( \frac{\sigma_n^2}{\text{sum}(\sigma^2)} \right)^{-1}, \quad (14)$$

where the first term is the Euclidean distance and the second term represents the inverse of the normalised variance. This weighted distance term discourages the model from causing high regression residuals with low uncertainty and attenuates the loss when having high uncertainty. The regulariser is defined by

$$\mathcal{R} = \frac{1}{N} \sum_{n=1}^N \ln \sigma_n^2. \quad (15)$$

This regularisation term is designed to penalise a high amount of uncertainty, thereby preventing the model from inactive learning.

### III. EXPERIMENTS

The primary purpose of our experiments is to identify the contribution made by Bayesian uncertainty analysis, benchmarked against a non-Bayesian approach (i.e. a predictive model without an uncertainty analyser).

#### A. Experimental Setup

Our implementation is based primarily on a prior art [25]. The residual dense network (RDN) architecture, which has its origin in low-level computer vision, is used for the experiments [38]. The neural network is trained on the BOSSbase dataset [39], consisting of 10,000 greyscale photographs collected for an academic competition for digital steganography. The inference set comprises standard test images from the USC-SIPI dataset [40]. The dropout rate is set to 0.3, the regularisation rate  $\lambda$  to 1, and the number of dropout samples  $T$  to 1,000 empirically. Pseudo-random messages are embedded into residuals whose absolute magnitudes are equal to or less than 2 (i.e.  $\alpha = 3$ ) with approximately 1.5 bits embedded into each residual of magnitude 0 and 1 bit into that of magnitude  $\pm 1$  or  $\pm 2$ .

#### B. Experimental Results

Figures 3 and 4 visualise the experimental results. The metrics used for measuring the quality of predicted images are peak signal-to-noise ratio (PSNR) and structural similarity (SSIM). In general, prediction performance is high for smooth images and low for richly textured images. The chequerboard artefacts are observed in the uncertainty maps since a chequered pattern (derived from 4-connectivity) is used for context-query splitting and the intensities of context pixels in an input image are consistent with those in a corresponding target image. The results suggest that the model is capable of eliminating uncertainty about the context pixels. It can be seen that uncertainty is concentrated around edges, contours, rare patterns, and textural details. Figure 5 depicts uncertainty quantification performance, represented by the root-mean-square error (RMSE) vis-à-vis the percentage of pixels. It illustrates the deviation of predictions as the percentage of pixels increases, where the pixels are selected in ascending order of uncertainty magnitude. The upper bound is obtained by selecting pixels in ascending order of residual magnitude, whereas the lower bound is computed by selecting

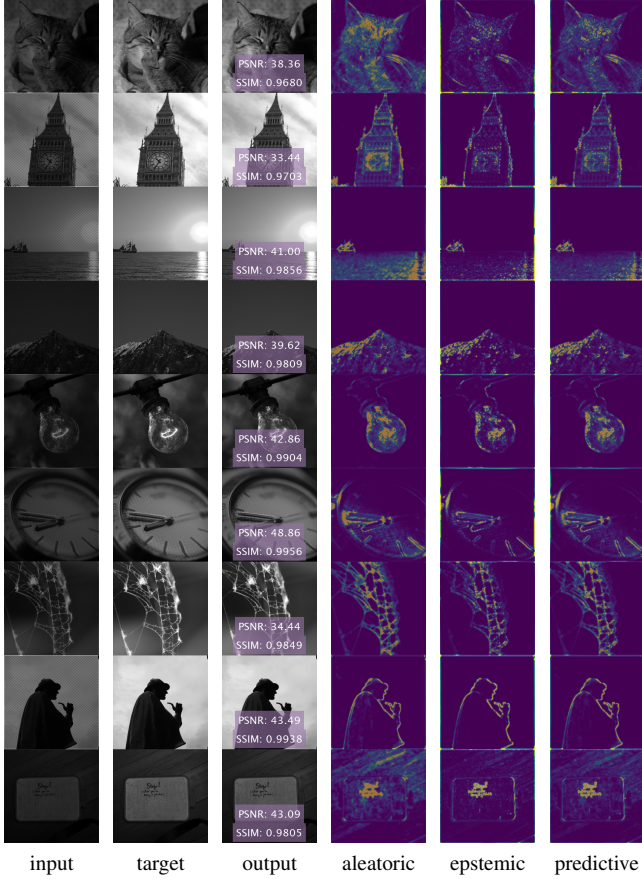


Fig. 3: Visual results from BOSSbase dataset.

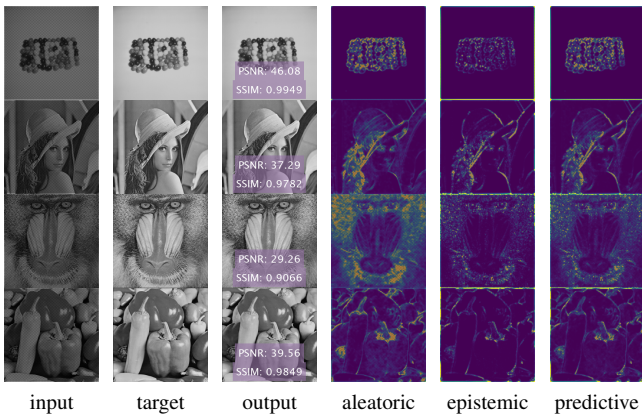


Fig. 4: Visual results from USC-SIPI dataset.

pixels in random order. The results verify the validity of uncertainty analysis by comparing it with a baseline of random selection. Figure 6 evaluates steganographic performance by the capacity-distortion curves. Capacity is measured by the embedding rate expressed in bits per pixel (bpp) and distortion is measured by the PSNR expressed in decibels (dB). The results show that Bayesian uncertainty analysis leads to a better trade-off between capacity and distortion.

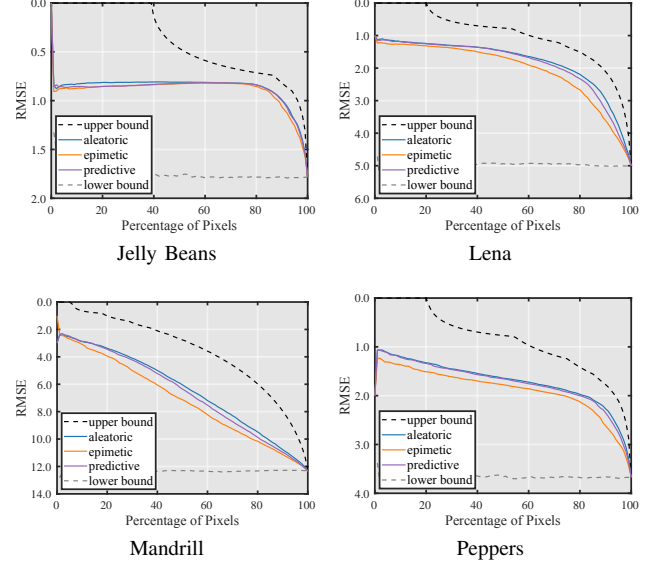


Fig. 5: Uncertainty quantification performance by RMSE vs percentage of pixels.

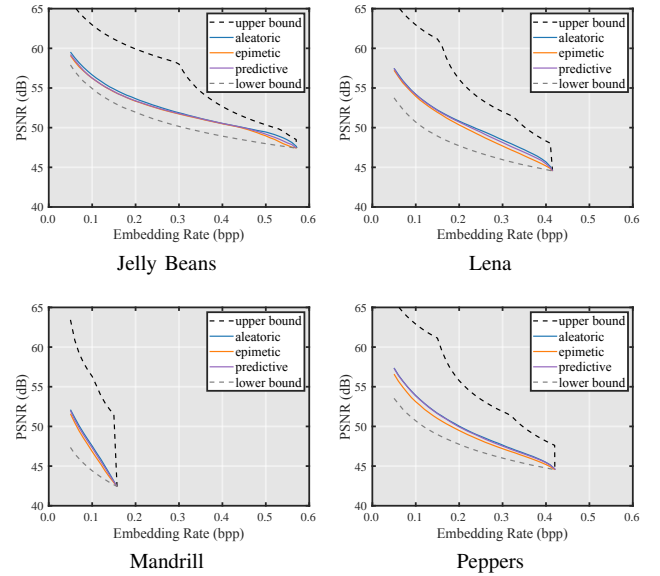


Fig. 6: Steganographic performance by PSNR vs embedding rate.

#### IV. CONCLUSION

In this letter, we study reversible steganography with deep learning and analyse uncertainty in predictive models based upon a Bayesian framework. We apply the Monte Carlo dropout to approximate the predictive distribution and derive aleatoric and epistemic uncertainties therefrom. A dual-headed neural network is constructed for estimating uncertainty in an unsupervised manner. Experimental results demonstrate state-of-the-art steganographic performance benchmarked against a non-Bayesian baseline, confirming the contribution of uncertainty analysis. We hope this article can shed light on future research of reversible steganography and envisage further progress ushered in with new developments of Bayesian deep learning.

## REFERENCES

- [1] A. M. Turing, "Computing machinery and intelligence," *Mind*, vol. LIX, no. 236, pp. 433–460, 1950.
- [2] A. Krizhevsky, I. Sutskever, and G. E. Hinton, "ImageNet classification with deep convolutional neural networks," in *Proc. Int. Conf. Neural Inf. Process. Syst. (NeurIPS)*, Lake Tahoe, NV, USA, 2012, pp. 1097–1105.
- [3] K. Simonyan and A. Zisserman, "Very deep convolutional networks for large-scale image recognition," in *Proc. Int. Conf. Learn. Representations (ICLR)*, San Diego, CA, USA, 2015, pp. 1–14.
- [4] Y. LeCun, Y. Bengio, and G. Hinton, "Deep learning," *Nature*, vol. 521, no. 7553, pp. 436–444, 2015.
- [5] R. McAllister, Y. Gal, A. Kendall, M. van der Wilk, A. Shah, R. Cipolla, and A. Weller, "Concrete problems for autonomous vehicle safety: Advantages of Bayesian deep learning," in *Proc. Int. Joint Conf. Artif. Intell. (IJCAI)*, Melbourne, Australia, 2017, pp. 4745–4753.
- [6] H. Wang and D.-Y. Yeung, "A survey on Bayesian deep learning," *ACM Comput. Surv.*, vol. 53, no. 5, pp. 108:1–37, 2020.
- [7] F. A. P. Petitcolas, R. J. Anderson, and M. G. Kuhn, "Information hiding—A survey," *Proc. IEEE*, vol. 87, no. 7, pp. 1062–1078, 1999.
- [8] J. Fridrich, M. Goljan, and R. Du, "Invertible authentication," in *Proc. SPIE Conf. Secur. Watermarking Multimedia Contents (SWMC)*, San Jose, CA, USA, 2001, pp. 197–208.
- [9] J. Tian, "Reversible data embedding using a difference expansion," *IEEE Trans. Circuits Syst. Video Technol.*, vol. 13, no. 8, pp. 890–896, 2003.
- [10] Z. Ni, Y.-Q. Shi, N. Ansari, and W. Su, "Reversible data hiding," *IEEE Trans. Circuits Syst. Video Technol.*, vol. 16, no. 3, pp. 354–362, 2006.
- [11] S. Lee, C. D. Yoo, and T. Kalker, "Reversible image watermarking based on integer-to-integer wavelet transform," *IEEE Trans. Inf. Forensics Secur.*, vol. 2, no. 3, pp. 321–330, 2007.
- [12] Y.-Q. Shi, X. Li, X. Zhang, H. Wu, and B. Ma, "Reversible data hiding: Advances in the past two decades," *IEEE Access*, vol. 4, pp. 3210–3237, 2016.
- [13] X. Duan, K. Jia, B. Li, D. Guo, E. Zhang, and C. Qin, "Reversible image steganography scheme based on a U-Net structure," *IEEE Access*, vol. 7, pp. 9314–9323, 2019.
- [14] K.-H. Jung, Z. Zhang, G. Fu, F. Di, C. Li, and J. Liu, "Generative reversible data hiding by image-to-image translation via GANs," *Secur. Commun. Netw.*, vol. 2019, pp. 4932782:1–10, 2019.
- [15] C.-C. Chang, "Adversarial learning for invertible steganography," *IEEE Access*, vol. 8, pp. 198425–198435, 2020.
- [16] S.-P. Lu, R. Wang, T. Zhong, and P. L. Rosin, "Large-capacity image steganography based on invertible neural networks," in *Proc. IEEE/CVF Conf. Comput. Vis. Pattern Recognit. (CVPR)*, virtual, 2021, pp. 10816–10825.
- [17] C. E. Shannon, "A mathematical theory of communication," *Bell Syst. Tech. J.*, vol. 27, no. 3, pp. 379–423, 1948.
- [18] M. U. Celik, G. Sharma, A. M. Tekalp, and E. Saber, "Lossless generalized-LSB data embedding," *IEEE Trans. Image Process.*, vol. 14, no. 2, pp. 253–266, 2005.
- [19] D. M. Thodi and J. J. Rodriguez, "Expansion embedding techniques for reversible watermarking," *IEEE Trans. Image Process.*, vol. 16, no. 3, pp. 721–730, 2007.
- [20] V. Sachnev, H. J. Kim, J. Nam, S. Suresh, and Y.-Q. Shi, "Reversible watermarking algorithm using sorting and prediction," *IEEE Trans. Circuits Syst. Video Technol.*, vol. 19, no. 7, pp. 989–999, 2009.
- [21] X. Li, B. Yang, and T. Zeng, "Efficient reversible watermarking based on adaptive prediction-error expansion and pixel selection," *IEEE Trans. Image Process.*, vol. 20, no. 12, pp. 3524–3533, 2011.
- [22] I. Dragoi and D. Coltuc, "Local prediction based difference expansion reversible watermarking," *IEEE Trans. Image Process.*, vol. 23, no. 4, pp. 1779–1790, 2014.
- [23] R. Hu and S. Xiang, "CNN prediction based reversible data hiding," *IEEE Signal Process. Lett.*, vol. 28, pp. 464–468, 2021.
- [24] C.-C. Chang, "Neural reversible steganography with long short-term memory," *Secur. Commun. Netw.*, vol. 2021, pp. 5580272:1–14, 2021.
- [25] C.-C. Chang, X. Wang, S. Chen, I. Echizen, V. Sanchez, and C.-T. Li, "Deep learning for predictive analytics in reversible steganography," arXiv, 2022.
- [26] Y. Gal, "Uncertainty in deep learning," Ph.D. dissertation, Dept. Eng., Uni. Cambridge, Cambridge, UK, 2016.
- [27] E. B. Wilson, "First and second laws of error," *J. Amer. Statist. Assoc.*, vol. 18, no. 143, pp. 841–851, 1923.
- [28] G. E. Hinton and D. van Camp, "Keeping the neural networks simple by minimizing the description length of the weights," in *Proc. Annu. Conf. Comput. Learn. Theory (COLT)*, Santa Cruz, CA, USA, 1993, pp. 5–13.
- [29] M. I. Jordan, Z. Ghahramani, T. S. Jaakkola, and L. K. Saul, "An introduction to variational methods for graphical models," *Mach. Learn.*, vol. 37, no. 2, pp. 183–233, 1999.
- [30] D. P. Kingma and M. Welling, "Auto-encoding variational Bayes," in *Proc. Int. Conf. Learn. Represent. (ICLR)*, Y. Bengio and Y. LeCun, Eds., Banff, AB, Canada, 2014, pp. 1–14.
- [31] A. Graves, "Practical variational inference for neural networks," in *Proc. Int. Conf. Neural Inf. Process. Syst. (NeurIPS)*, Granada, Spain, 2011, pp. 2348–2356.
- [32] C. Blundell, J. Cornebise, K. Kavukcuoglu, and D. Wierstra, "Weight uncertainty in neural networks," in *Proc. Int. Conf. Mach. Learn. (ICML)*, Lille, France, 2015, pp. 1613–1622.
- [33] Y. Gal and Z. Ghahramani, "Bayesian convolutional neural networks with Bernoulli approximate variational inference," in *Proc. Int. Conf. Learn. Represent. (ICLR)*, San Juan, PR, USA, 2016, pp. 1–12.
- [34] N. Srivastava, G. Hinton, A. Krizhevsky, I. Sutskever, and R. Salakhutdinov, "Dropout: A simple way to prevent neural networks from overfitting," *J. Mach. Learn. Res.*, vol. 15, no. 56, pp. 1929–1958, 2014.
- [35] Y. Gal and Z. Ghahramani, "Dropout as a Bayesian approximation: Representing model uncertainty in deep learning," in *Proc. Int. Conf. Mach. Learn. (ICML)*, New York, NY, USA, 2016, pp. 1050–1059.
- [36] A. Kendall and Y. Gal, "What uncertainties do we need in Bayesian deep learning for computer vision?" in *Proc. Int. Conf. Neural Inf. Process. Syst. (NeurIPS)*, Long Beach, CA, USA, 2017, pp. 5580–5590.
- [37] D. Nix and A. Weigend, "Estimating the mean and variance of the target probability distribution," in *Proc. IEEE Int. Conf. Neural Netw. (ICNN)*, Orlando, FL, USA, 1994, pp. 55–60.
- [38] Y. Zhang, Y. Tian, Y. Kong, B. Zhong, and Y. Fu, "Residual dense network for image super-resolution," in *Proc. IEEE/CVF Conf. Comput. Vis. Pattern Recognit. (CVPR)*, Salt Lake City, UT, USA, 2018, pp. 2472–2481.
- [39] P. Bas, T. Filler, and T. Pevný, "Break our steganographic system: The ins and outs of organizing BOSS," in *Proc. Int. Workshop Inf. Hiding (IH)*, Prague, Czech Republic, 2011, pp. 59–70.
- [40] A. G. Weber, "The USC-SIPI image database: Version 5," USC Viterbi School Eng., Signal Image Process. Inst., Los Angeles, CA, USA, Tech. Rep. 315, 2006.